

Characterization of electrodeposited Ni–MoS₂ composite coatings under the influence of current density

A. Gana^{a,*}, H. Ben Temam^a, F. Lekmine^{a,b}, M. Naoun^c, O. Herzallah^a

^aPhysics Laboratory of Thin Films and Applications (LPCMA), University of Biskra, Algeria

^bPhysics department, ABBES Laghrour Khenchela University P.O 1252, 40004, Algeria

^cCorrosion Laboratory, Mechanical Department, Faculty of Technology, Batna2 University, Algeria

In this paper, the influence of current density on electrodeposited Ni–MoS₂ composite coatings has been studied for the first time. Low carbon steel alloy has been selected as a substrate. The Ni–MoS₂ composite coatings are deposited at a temperature of 48 °C with applied current densities of (1, 2, 3 and 4 A/dm²). The x-ray diffraction (XRD) analysis of electrodeposited Ni–MoS₂ coatings depicts a number of sharp peaks indicating a good crystallinity. Using ASTM database, the peaks at 14°, 32°, 33°, 39°, 49° and 58° correspond to (200), (100), (101), (103), (105) and (110) hkl planes respectively. The morphology was examined by scanning electron microscopy (SEM). Microhardness measurements show that all Ni–MoS₂ samples are harder than low carbon steel substrate. EDX analysis of the Ni–MoS₂ composite confirmed that the fraction of MoS₂ increased with the increase of applied current density. The study of corrosion properties was carried out in a 0.6M NaCl solution. The potentiodynamic polarization curve of electrodeposited Ni–MoS₂ confirmed that the corrosion resistance increases with the decrease of applied current density. In addition, Electrochemical tests show that the optimal value of applied current density is 3 A/dm² in the sense of the least value of $E_{\text{corr}} = -314,1$ mV and the best resistance was $R_p = 9.52$ K.cm².

(Received March 29, 2021; Accepted July 8, 2021)

Keywords: Ni–MoS₂, Deposition, Corrosion resistance, Low carbon steel, Polarization, EDX

1. Introduction

Due to their high resistance to wear and corrosion, nickel and nickel-based composites are largely used in a variety of electrochemical applications [1,2]. In different electrochemical processes, these composites exhibit a significant corrosion resistance combined with high catalytic activity under the action of aggressive solution [3]. It is well known that the electrodeposition method, the electric current is conveyed across an electrolyte. As a result, the metallic ions are deposited at the cathode [4]. The electrodeposition process offer several advantages over other deposition techniques [5,6]. The production of composite plating can be performed by the use of highly dispersed fine particles in the metal plating electrolyte. The dispersed particles will be trapped in the deposit. This process is called electrodeposition or composite deposition [6]. Currently, this electrodeposition technique of solid particles in metallic martix has been widely used in a variety application such as piezoelectrical devices, fuel cells, biomedical implants, solar cells, super capacitors, and in other surface modifications and protections [7]. Recently, there has been a growing interest in reducing the friction and wear problems for critical mechanical parts in both the advanced automobile and aerospace applications. To this end, nickel-based composite coatings have been developed with embedded MoS₂ to bring the sought after solutions to friction and wear issues [8,9]. The particles are mainly selected from a wide span of materials ranging from metallic elements, powders and oxide powders of Ni, Cu, Al, Si, Co, In, Sn, V, Mg and Zn. Similarly, nitrides of B, Al, Si as well as carbon C (graphite or diamond) and carbides of Bi, Si, B, W and MoS₂ and organic compounds such as polytetrafluoroethylene (PTFE) and polymer

* Corresponding author: alb187954@gmail.com

spheres. Therefore, the nickel-base composite coating Ni–MoS₂ is a key material for a wide span of engineering aspects. In this paper, we study the effect of plating deposition current density on the Ni–MoS₂ electrodeposited coatings. In addition, this work aims to develop electroless plating of nickel-based composite Ni–MoS₂ coatings to achieving high hardness and low corrosion.

2. Experimental

2.1. Electrodeposition of Ni–MoS₂ coatings

In our experiment, Ni–MoS₂ coatings were electrodeposited on low carbon steel sheet substrate which was polished using (120-1200) grit silicon carbide papers, washed with detergents to remove any oil residue, dried with a paper towel then activated in 10% wt/vol hydrochloric acid for 10 seconds to remove any oxide films and to obtain an active fresh surface. The substrate was rinsed in purified water before electrodeposition. This pre-treatment ensured a good adhesion between the coating and the substrate. The chemical composition of the substrate is given in Table 1. The electrolytes contained nickel sulfate (NiCl₂·6H₂O), molybdenum disulfide (MoS₂), sodium chloride (NaCl), ammonium chloride (NH₄Cl), and boric acid (H₃BO₃) as shown in Table 2. Distilled water was used to prepare the electrolyte solutions. The pH of the solution was adjusted by addition of aqueous HCl or NaOH solutions. Low carbon steel 10 × 5.55 × 2.5 mm³ sheet substrates were used as cathode and the anode was a nickel sheet. In order to remove oil and greases prior to deposition, the substrates were degreased using a solution containing (NaOH 0.375 mol/l, Na₂CO₃ 0.472 mol/l) then were pickled in (10 %) HCl solution to remove oxide traces. On the other hand, Ni–MoS₂ coatings were deposited at different plating current densities namely; 1, 2, 3, and 4 A/dm². The electrodeposition was carried out at (48 ± 1) °C, pH (4 ± 0.5) during 60 min. The stirring speed was the same for all tests.

Table 1. Chemical composition of the substrate.

Elements	C	Mn	Si	S	P	Al
Content (wt %)	0.15	0.75	0.02	0.015	0.012	0.043

Table 2. Electrolyte composition and working conditions of Ni–MoS₂ electrolyte.

Electrolyte	Concentration (g/l)	Conditions	
NiCl ₂ ·6H ₂ O	22.5	pH	4
NH ₄ Cl	21.4	Temperature	48 °C
H ₃ BO ₃	18.6	Current density	1, 2, 3, and 4 A/dm ²
NaCl	5.85	Type of current	Direct (DC)
MoS ₂ powder	5	Agitation of electrolyte	Magnetic stirring

2.2. Surface characterizations

2.2.1. Adherence test

To evaluate the adherence of Ni–MoS₂ composite coatings, the coated samples were heated at 250 °C for 30 min and quenched in water at ambient temperature [10].

2.2.2. Physical and Hardness characterizations

X-Ray Diffraction characterization of samples was carried out using a D8 Advance-Brucker with Cu-K α radiation ($\lambda = 0.15406$ nm) and 0.03° as 2 θ step. The surface morphology of different Ni–MoS₂ deposits was observed by a JEOL JSM 5800 scanning electron microscope (SEM). The compositions of Ni–MoS₂ coatings were determined with energy dispersive X-ray spectroscopy (EDS)

analysis tool attached to SEM. Microhardness testing of coatings was performed by Vickers hardness tester Wolpert Wilson Instruments (model 402MVD). The load was applied under a charge of 50g during 10 second, and the average of ten hardness measurements was quoted as the hardness value.

2.2.3. Electrochemical tests

Potentiodynamic polarization measurements were carried out using a standard three-electrode cell, the coated sample (1 cm^2) was set as working electrode, Pt as auxiliary electrode and saturated calomel electrode as a reference electrode. All these electrodes were immersed in 3.5 wt% NaCl electrolyte. The cell was connected to Voltalab 20 (PGP201) device working at a scanning rate of 0.25 mV/s and in a potential range from -800 to 200 mV. Corrosion rate (mm/y), corrosion potential E_{corr} (mV), and Tafel slopes (mV/s) were calculated with extrapolation technique provided by Volta Master 4 software.

3. Results and discussions

3.1. Physical characterization

3.1.1. X-ray diffraction

Fig. 1 gives X-ray diffraction patterns of the coatings obtained at different current densities. According to Ni–MoS₂ phase diagram and previous researches [11].

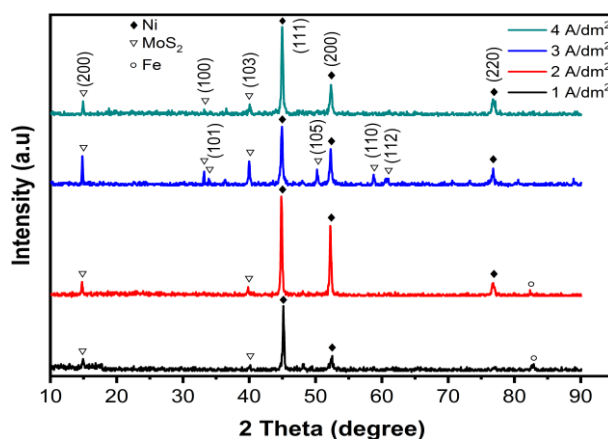


Fig. 1. XRD patterns of Ni–MoS₂ alloys deposits as a function of applied current density.

XRD diagram illustrates a number of sharp peaks which indicative of good crystallinity. At a current density of 3 A/dm^2 , the peaks appeared at $2\theta = 14^\circ, 32^\circ, 33^\circ, 39^\circ, 49^\circ, 58^\circ$ and 60° correspond to the planes (002), (100), (101), (103), (105), (110) and (112) respectively, Which reveal the structure of MoS₂. The appearance of all these peaks corresponds to the increase in the MoS₂ content in the deposit (Fig. 3). We also note the effect of changing the current density on the crystallization of the MoS₂ composite coating. At current density values of 1, 2, and 4 A/dm^2 , planes (101), (105), (110) and (112) did not appear, and this is due to the decline content of MoS₂ in the deposit (Fig. 3). The results also indicate that the electrochemical technique improves the action of Ni ions in enhancing the crystallinity and the deposition of the MoS₂ [12,13].

3.1.2. EDX analysis of the Ni–MoS₂ composite coating

The chemical compositions of Ni–MoS₂ alloy at different applied current densities are depicted in Fig. 2.

Fig. 3 illustrates the variation of MoS₂ content in the deposit versus the applied current density. The MoS₂ content in the deposit varies with the increase of applied current density. We noticed that when increasing the current density from 1 A/dm^2 to 3 A/dm^2 , the MoS₂ content in the deposit increases from Mo (0.92 wt%), S (0.42 wt%) to Mo (2.7 wt%), S (2.01 wt%), respectively this

behavior is probably due to the rise in the movement of the MoS_2 particles towards the cathode as a consequence of current density variation. On the other hand when the current density increases to a value of 4 A/dm^2 the MoS_2 content in the deposit decreases from Mo (2.7 wt%), S (2.01 wt%) to Mo (2.4 wt%), S (1.28 wt%), this is offset by the increased rates of deposition of nickel ions from 95.2 wt% to 96.27 wt%. During the deposit process, the deposition rate of nickel ions becomes faster than MoS_2 particles when the current density reaches the value 4 A/dm^2 . This fact results from the reduction of MoS_2 content [14].

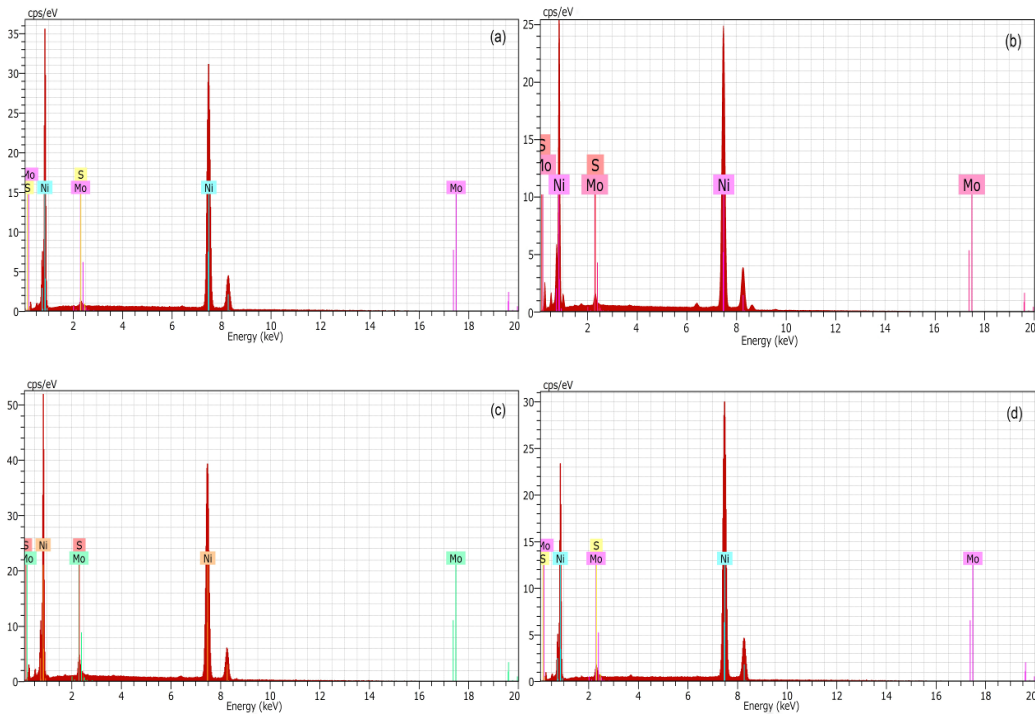


Fig. 2. EDX analysis of (a) Ni-MoS_2 (1 A/dm^2), (b) Ni-MoS_2 (2 A/dm^2), (c) Ni-MoS_2 (3 A/dm^2), (d) Ni-MoS_2 (4 A/dm^2) Composite coatings deposited at $T = 48 \text{ }^\circ\text{C}$ and $\text{pH } 4$ for 60 min.

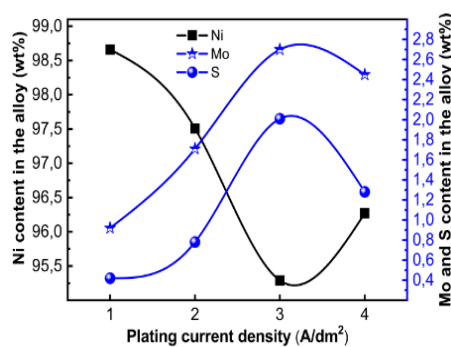


Fig. 3. Influence of the applied current density on the composition of Ni and MoS_2 in Ni-MoS_2 composite plating.

3.1.3. Surface morphology

SEM inspection revealed features of the microscopic surface roughness on Ni-MoS_2 composite coatings (Fig. 4). We observe the dendrite growth of Ni-deposited MoS_2 on all coatings. Done first, MoS_2 particles are incorporated into the deposited Ni film layer. Ni is electrodeposited on both the substrate and the incorporated MoS_2 particles because of their high electrical conductivity. The electrodeposited Ni is deposited on the outer surface of MoS_2 particles building an external layer that

surrounds them. Meanwhile, MoS_2 particles are more easily captured on protruding ends of the MoS_2 incorporated into electrodeposited Ni than on the substrate. This fact leads to dendrite growth of Ni- MoS_2 composite [15].

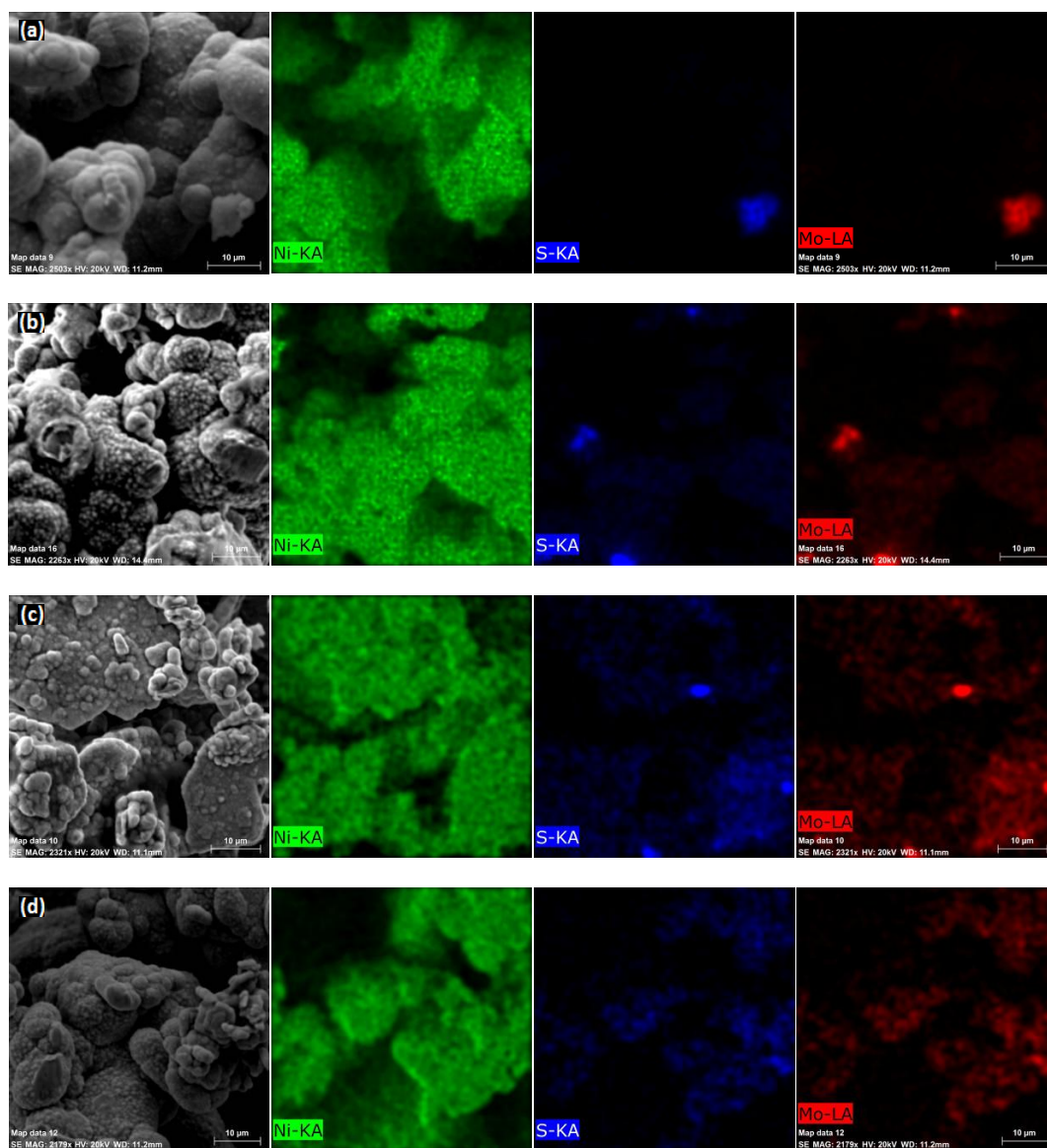


Fig. 4. SEM images and Graphic card of Ni- MoS_2 coatings electrodeposited at: (a) 1 A/dm^2 , (b) 2 A/dm^2 , (c) 3 A/dm^2 and (d) 4 A/dm^2 .

Screening mapping by EDX revealed a uniform distribution of nickel in the composite coatings as shown in Fig.4 (a, b, c) and (d). The distribution of the Mo and S contents (as an indicator of the presence of MoS_2) was more concentrated in the surface protrusion structures, and more scattered over the surface at the current density 3 A/dm^2 as shown in Fig.4 (c).

3.1.4. Micro-hardness testing

It is obvious from Fig. 5 that the hardness values increase with increasing electrodeposition current density from 1 A/dm^2 to 3 A/dm^2 . This corresponds to the increase of MoS_2 content. The hardness of Ni- MoS_2 composite coatings deposit is 302 HV after deposition at 3 A/dm^2 which is greater than the one deposited at 1 A/dm^2 (241 HV). This fact can be attributed to the dispersion strengthening effect [15]. However, the hardness decreases with an increase of the current density from

3 A/dm² to 4 A/dm² and this can be attributed to the decrease of MoS₂ content. Additionally, we find that molybdenum disulfide is harder than low carbon steel substrate (Table 3).

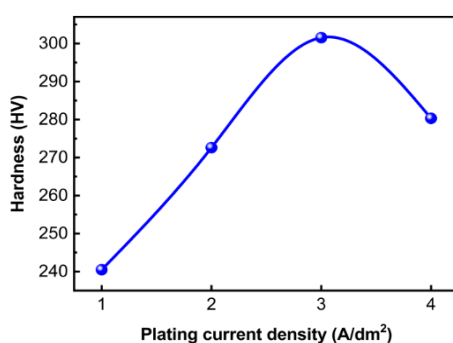


Fig. 5. Vickers microhardness of composite coatings vs the plating current density (A/dm²).

Table 3. Values of micro-hardness Vickers hardness (HV) registered different current density.

Plating current density (A/dm ²)	Hardness (HV)
1	240.5
2	272.63
3	301.55
4	280.33
Substrate	147.3

3.2. Electrochemical characterization

3.2.1. Potentiodynamic polarization studies

Fig. 6 gives the potentiodynamic polarization curves of the different studied coatings. The electrochemical parameters are evaluated using the Tafel extrapolation method. Electrochemical results are summarized in Table 4.

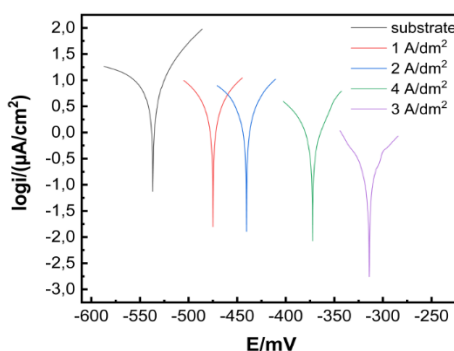


Fig. 6. Polarization curves of Ni–MoS₂ deposited composites at different current densities.

It is clearly seen Fig. 6 and Table 4 that a nobler Ni–MoS₂ alloy coating electroplated at 3 A/dm² has the highest corrosion resistance value $R_p = 9,52 \text{ K}\Omega.\text{cm}$ and the lowest corrosion potential $E_{\text{corr}} = -314,1 \text{ mV}$. Therefore, the obtained results showed a great potential to improve electrochemical behavior of low carbon steel substrate and are ready to be put in practice.

Table 4. Corrosion parameters of electrodeposited Ni–MoS₂ composites at different plating current densities

Plating current density (A/dm ²)	E _{corr} (mV)	I _{corr} (μA/cm ²)	R _p (KΩ.cm ²)
substrate	-536,6	9,8498	1,43
1	-474,9	3,4155	2,96
2	-440,4	2,8204	3,41
3	-314,1	1.0401	9.52
4	-372,4	2,0236	7,89

4. Conclusion

In this work, we investigated the effects of electrodeposition current density on surface morphology, microstructure, electrochemical characteristic and the microhardness of Ni–MoS₂ composites.

Thermal shock testing suggests a good adherence between deposited Ni–MoS₂ coating and low carbon steel substrate. The surface morphology of each coating exhibited surface dendrite growth that is tightly dependent on the applied current density.

The XRD analysis showed the presence of a crystalline structure with preferred growth orientations (002) and (111). Electrochemical tests suggested an optimal value of applied current density of 3 A/dm² in a sense of the lowest corrosion rate and the least value of E_{corr}. Microhardness test showed that Ni–MoS₂ alloy coating is harder than low carbon steel substrate.

Acknowledgments

I would like to thanks "Responsible of Physics Laboratory of Thin Films and Applications (LPCMA)" and "Responsible of Corrosion Laboratory, Mechanical Department, Faculty of Technology, Batna2 University" for their assistance in the preparation of this work.

References

- [1] L. Burzyńska, E. Rudnik, Hydrometallurgy **54**, 133 (2000).
- [2] D. Golodnitsky, Y. Rosenberg, A. Ulus, Electrochim. Acta **47**, 2707 (2002).
- [3] J. Kubisztal, A. Budniok, Int. J. Hydrogen Energy **33**, 4488 (2008).
- [4] J. B. Mohler, H. J. Sedusky, Electroplating for the Metallurgist, Engineer, and Chemist (Chemical Publishing Company, New York, 1951).
- [5] I. Gurrappa, L. Binder, Sci. Technol. Adv. Mater. **9**, (2008).
- [6] J. L. Stojak, J. Fransaer, J. B. Talbot, in *Adv. Electrochem. Sci. Eng. Vol. 7* (Wiley-VCH Verlag GmbH, Weinheim, FRG, 2001), p. 193.
- [7] I. Zhitomirsky, Surf. Eng. **27**, 403 (2011).
- [8] E. S. S. Güler, E. Konca, I. İ. Karakaya, Int. J. Surf. Sci. Eng. **11**, 418 (2017).
- [9] Z. Li, J. Wang, J. Lu, J. Meng, Appl. Surf. Sci. **264**, 516 (2013).
- [10] H. Ben Temam, A. Chala, S. Rahmane, Surf. Coatings Technol. **205**, S161 (2011).
- [11] N. Zhou, S. Wang, F. C. Walsh, Electrochim. Acta **283**, 568 (2018).
- [12] D. Wang, X. Zhang, Y. Shen, Z. Wu, RSC Adv. **6**, 16656 (2016).
- [13] Y. C. Xie, Y. M. Li, Adv. Mater. Res. **871**, 206 (2014).
- [14] S. L. Kuo, J. Chinese Inst. Eng. Trans. Chinese Inst. Eng. A/Chung-Kuo K. Ch'eng Hsueh K'an **27**, 243 (2004).
- [15] Z. Huang, D. Xiong, Surf. Coatings Technol. **202**, 3208 (2008).